ATLANTIS PRESS

Advances in Engineering Research, volume 155

2nd International Conference on Advances in Energy, Environment and Chemical Science (AEECS 2018)

One Pot Hydrothermal Synthesis of $ZnFe_2O_4$/rGO with Enhanced Photoelectrochemical Performance for Water Splitting

Yue He[1], Yan Zhang[*], Fengkai Yu[1], Linlin Zhang[1], and Jianqiang Yu[1, 2, *]

[1]*Institute of Green Chemistry and Industrial Catalysis, School of Chemistry and Chemical Engineering, Qingdao University, 308 Ningxia Road, Qingdao, China*

[2] *Qingdao Center of Resource Chemistry and New Material, Lanzhou Institute of Chemical Physics, Chinese Academy of Sciences, Qingdao,China*

jianqyu@qdu.edu.cn

Keywords: Photoelectrochemical Water Splitting; $ZnFe_2O_4$/rGO; Hydrothermal Process; High Efficiency

Abstract: Spinel structure of $ZnFe_2O_4$ has attracted widespread attention due to its excellent visible-light-driven photocatalytic activity. The composite photocatalyst of $ZnFe_2O_4$ and reduced graphene oxide (rGO) have been synthesized by a facile one-step hydrothermal strategy. A substantially enhanced photoelectrochemical activities for water splitting compared to pure $ZnFe_2O_4$ under visible light irradiation were observed. However, as the content of graphene in the composite increased, $ZnFe_2O_4$ nanoparticles gradually accumulate to cluster particles, which is not good for the improvement of photoelectrochemical activities.

1 INTRODUCTION

Many problems caused by energy shortage and environmental pollution have made it urgent for all countries in the world to find renewable, efficient and clean energy sources.[1, 2] Semiconductor photocatalysts can not only convert solar energy into electricity and chemical energy, but also can degrade organic pollutants into small molecule inorganic substances.[3]

$ZnFe_2O_4$ (ZFO) has received intensive attention due to its excellent magnetic properties and stable chemical properties. Its band-gap is around 1.9 eV, which is appropriate for the visible light absorption. $ZnFe_2O_4$ showed good oxidative decomposition over different kinds of organic contaminants under visible light.[4] Reduced graphene oxide (rGO) was widely noted as an ideal adsorbent and a good substrate for anchoring inorganic materials. Numerous attempts have been made to combine graphene with semiconductor photocatalysts to enhance their photocatalytic performance, but very few researches on the photo-to-current conversion property over graphene and $ZnFe_2O_4$ composite photoelectrode has been reported.[5, 6]

In this work, we have successfully developed a facile and effective one-pot hydrothermal process to synthesize ZFO/rGO composite material under the presence of graphene oxide (GO). The results indicate that the presence of rGO enhanced the conductivity of the composite materials and thereby reduced the possibility of surface charges recombination.

2 EXPERIMENTS

2.1 Materials

Graphite was purchased from Tianjin Institute of Chemical Reagents (Tianjin). $Zn(NO_3)_2{\cdot}6H_2O$(99%), $Fe(NO_3)_3{\cdot}9H_2O$(99%), $KMnO_4$, H_3PO_4, H_2O_2 (30%), HCl (35%), NH_3H_2O (25%) were purchased from Sinopharm Chemical Reagent Co., Ltd. All reactants and solvents were analytical grade and used without further purification. Distilled water was purified by Flom ultrapure water system.

2.2 Characterization

Powder X-ray diffraction (XRD) was used to examine the crystalline phase of the products. Diffraction patterns of the samples were obtained on a Bruker D8-advance X-ray diffractometer with Cu-$K\alpha$ radiation. Each sample was scanned through a 2θ range from 10-80° with a rate of 4° / min. Transmission electron microscopy (TEM) measurement was carried out on a JEOL-2010 TEM with an accelerating voltage of 200 kV.

2.3 Synthesis of GO

GO was synthesized by a modified Hummers' method.[7] Graphite (5 g) was slowly added into the three-neck bottle containing 225 mL concentrated sulfuric acid and 25 mL phosphoric acid under stirring in the ice bath. Then, 35 g of $KMnO_4$ was slowly added into the above solution under vigorous stirring for 30 min. The aqueous was heated to 50℃ for 12 h and then cooled to room temperature. Subsequently, the paste poured into the ice step by step in the beaker. Then, appropriate H_2O_2 was added under stirring until the mix changing into light yellow. Finally, the mix was centrifuged and washed with hydrophobic acid, deionized water and ethanol several times and dried.

2.4 Synthesis of pure $ZnFe_2O_4$

1 mmol $Zn(NO_3)_2{\cdot}6H_2O$ and 2 mmol $Fe(NO_3)_3{\cdot}9H_2O$ were dissolved into 50 mL distilled water under stirring for 30 min. Then, NH_3H_2O (25%) was dripped into the above solution until the pH value increased to 9 and kept continuously stirring for 30 min. After that, the resulting suspensions were charged into PTFE-lined stainless autoclaves respectively and kept at 180 ℃ for 12 h. Subsequently, the autoclaves were cooled to room temperature naturally. The suspensions were centrifuged and washed with distilled water for several times and dried at 70℃ for 10 h.

2.5 Synthesis of pure $ZnFe_2O_4$/rGO

Different amounts of GO (2.43 mg, 4.92 mg, 7.45 mg, 10.04mg) were dispersed in 20mL distilled water respectively by ultrasonic for 1 h. The as-prepared solutions (1 mmol $Zn(NO_3)_2{\cdot}6H_2O$, 2 mmol $Fe(NO_3)_3{\cdot}9H_2O$, 30 mL) were added into the dispersions by dropwise under stirring for 1 h. Then the following operation is the same as the above. $ZnFe_2O_4$ powder containing 1%, 2%, 3%, 4% (weight percentage) GO were obtained.

2.6 Photocatalytic Performance

The photocatalytic properties of the samples were evaluated by degradation of Rhodamine B (RhB) under visible-light illumination. 20 mg of photocatalyst was added into the aqueous solution of RhB (5 mg / L, 40 mL) under stirring. Before irradiation, the suspensions were stirred in the dark for about 60 min to establish adsorption-desorption equilibrium. Subsequently, the suspensions were exposed to the visible-light irradiation from 800 W Xe lamp equipped with an ultraviolet cutoff filter (λ> 420 nm) after adding 1 mL H_2O_2 (30%) in it under stirring. The distance of about 10 cm was kept between the light source and the solution. The solution (4 mL) of the sample was taken out at a given time interval of 30 min during the experiment and centrifuged to remove the catalyst completely. The absorbance of RhB was recorded by UV-vis spectrophotometer at λ_{max} = 552 nm every interval.

3 RESULTS AND DISCUSSIONS

3.1 Structure and morphology

The crystal structures of the pure phase $ZnFe_2O_4$ and $ZnFe_2O_4$/rGO composites with different weight ratios of GO were analyzed by X-ray diffraction (XRD) pattern and shown in Figure1. All the diffraction peaks can be assigned to $ZnFe_2O_4$ (JCPDS No.22-1012), demonstrating that single-phase $ZnFe_2O_4$ samples were obtained. It was observed that the products exhibited a strong and sharp diffraction peaks, indicating a high crystalline by hydrothermal methods. No typical

diffraction peaks of rGO are observed in the XRD patterns for $ZnFe_2O_4$/rGO composites due to the relatively less amount of rGO on the surface.[8]

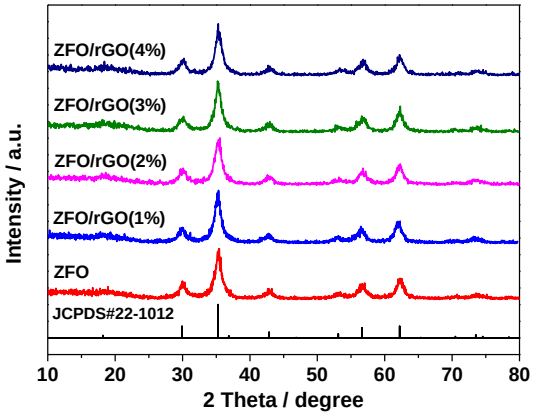

Figure 1. XRD patterns of $ZnFe_2O_4$ and $ZnFe_2O_4$/rGO composites with different weight ratios of GO

The morphologies of the pure phase $ZnFe_2O_4$ and $ZnFe_2O_4$/rGO composites with different weight ratios of GO were characterized by TEM. As shown in Figure 2(a-e), it can be observed that the morphologies of the pure phase $ZnFe_2O_4$ and $ZnFe_2O_4$ in $ZnFe_2O_4$/rGO composites are nano-sheets in the range of 8 to 14 nm. The pure phase $ZnFe_2O_4$ nanosheets are uniformly distributed. With the increase of weight ratios of GO, $ZnFe_2O_4$ nano-sheets began to cluster in the composites. High-resolution transmission electron microscopy (HRTEM) measurement was applied to supply the internal microstructure information on the as-prepared $ZnFe_2O_4$ nano-sheets. The lattice fringes could be apparently observed from Figure 2f, and constant value of the inter planar spacing between the adjacent lattice fringes were 0.255 nm, which was consistent with (311) planes of spinel $ZnFe_2O_4$. [9]

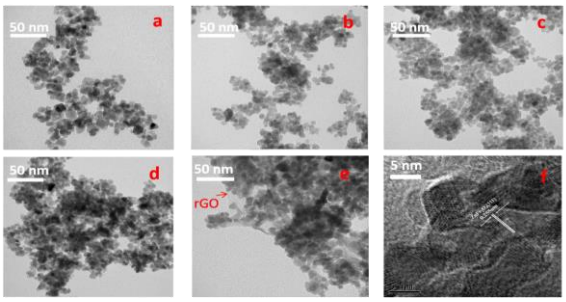

Figure 2. TEM images of (a) $ZnFe_2O_4$, (b) $ZnFe_2O_4$/rGO (1%), (c) $ZnFe_2O_4$/rGO (2%) , (d) $ZnFe_2O_4$/rGO (3.0%) , (e)$ZnFe_2O_4$/rGO(4%) and HRTEM images (f).

3.2 Raman and XPS analysis of $ZnFe_2O_4$/rGO composite

The Raman spectra of GO, pure phase $ZnFe_2O_4$ nano-sheets and $ZnFe_2O_4$/rGO (2%) composite were shown in Figure 3. For GO and $ZnFe_2O_4$/rGO (2%) composite, G band at about 1580 cm^{-1}, corresponding to an E_{2g} phonon mode of graphite, was attributed to the vibration of the sp^2-bonded carbon atoms, while D band atabout 1345 cm^{-1}, corresponding to a k-point phonon mode of A_{1g} symmetry, originates from the defects and disorder of carbonmaterials.[10]The Raman spectrum taken from the samples of pure phase $ZnFe_2O_4$ and $ZnFe_2O_4$/rGO (2%) composite showed two peaks at 349, and 656 cm^{-1}, which were consistent with the literature-reported values of $ZnFe_2O_4$ and $ZnFe_2O_4$/rGO composite.[11]

We could confirm that the GO was reduced to rGO by identifying the oxidation state of the C element. The X-ray photoelectron spectroscopy (XPS) (As shown in Figure 4) peak of C1s at 284.8 eV binding energy is assigned to C-C/C=C, indicating that most of the C atom is sp^2 hybridization, which indicated that the GO in the composite was reduced to rGO during the hydrothermal process.

3.3 Photocatalytic activity

The photoelectrochemical performances of pure phase $ZnFe_2O_4$ and $ZnFe_2O_4$/rGO composites photoelectrodes were investigated in a three-electrode photoelectron-chemical cell using a platinum foil as counter electrode and a Ag/AgCl as reference electrode under visible light (λ>420 nm). The working electrodes of the $ZnFe_2O_4$ and $ZnFe_2O_4$/rGO films were fabricated by the electrophoretic deposition. As shown in Figure 5, all the $ZnFe_2O_4$/rGO photoelectrodes showed much higher photocurrent density than the $ZnFe_2O_4$ photoelectrode. The $ZnFe_2O_4$/rGO photoelectrode with 2% rGO generates a photocurrent density of 49.9μA·cm^{-2}, which is 7.1 times higher than that of the $ZnFe_2O_4$ photoelectrode alone. Clearly, the Photoelectronchemical performance of $ZnFe_2O_4$/ rGO composite photoelectrode has been greatly enhanced. As such, both the electron accepting and transporting properties of graphene in the composite would contribute to the suppression of the charge recombination, and thereby enhancements in the photo-to-current conversion efficiency would be achieved. This result can also be verified by the electrochemical impedance technique to understand the role of rGO in the photoelectrochemical properties of the $ZnFe_2O_4$/rGO. Impedance measurements conducted on photoanode in 0.5 mol·L^{-1} of Na_2SO_4 electrolyte in the dark allowed the construction of Mott-Schottky plots of the $ZnFe_2O_4$ and $ZnFe_2O_4$/rGO with various ratios of GO.

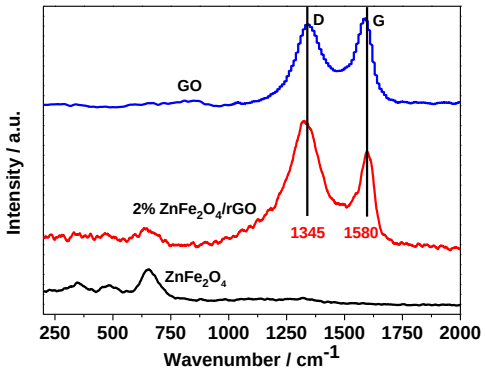

Figure 3. Raman spectra of GO, $ZnFe_2O_4$ nanoparticles, $ZnFe_2O_4$/rGO (2%) composite.

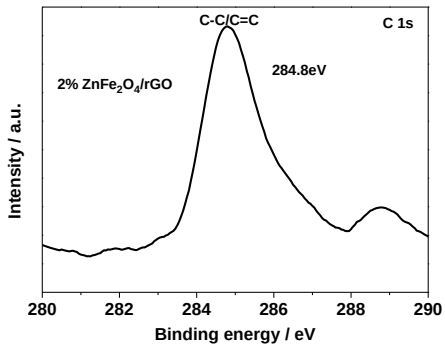

Figure 4. XPS spectrum of $ZnFe_2O_4$/rGO(2%)

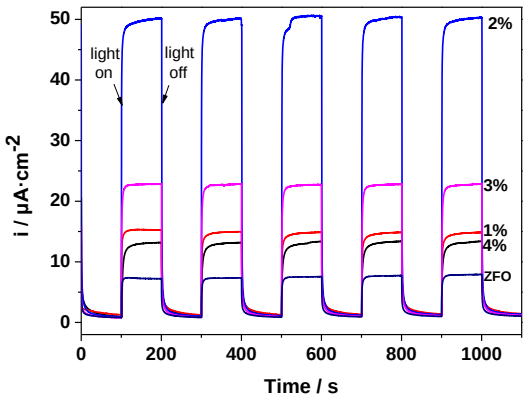

Figure 5. The photoinduced current densities of different photoanodes under intermittent visible light illumination. All curves were obtained at 0.20 V bias potential vs Ag/AgCl reference electrode.

As shown in Figure 6, the carrier density can be calculated by the slope of the Mott-Schottky curves. The lower the slope of a Mott-Schottky $ZnFe_2O_4$/rGO photoanodes showed a lower value of carrier density, clearly indicated a higher carrier density for $ZnFe_2O_4$/rGO photoanodes. An increased value of carrier density (ND) in semiconductors improves the charge conductivity, leading to an enhanced photoelectrochemical performance of the photoelectrode. Therefore, the increase in the carrier density was the main reason for the higher photocurrent of $ZnFe_2O_4$/rGO electrode. However, the slope increased with a further increase in graphene addition. However, the slope increased with a further increase in graphene addition (5.0%), indicating that the carrier density decreases.

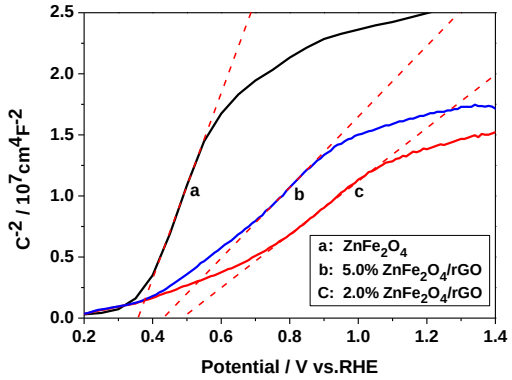

Figure 6. Mott–Schottky (MS) plots of ZFO and ZFO/rGO photoanodes measured in 0.1 M Na_2SO_4 (pH 6.3).

4 CONCLUSIONS

In summary, $ZnFe_2O_4$/rGO composite were successfully prepared by a facile one-step hydrothermal strategy. The presence of graphene oxide could significantly affect the electrochemical activity of $ZnFe_2O_4$ under visible light irradiation, and $ZnFe_2O_4$/rGO composites showed excellent photocatalytic activity.

REFERENCES

[1] Song F, Ding Y, Ma B, et al. Energy & Environmental Science, 2013, 6(4):1170-1184.

[2] Gupta V K, Kumar R, Nayak A, et al. Advances in Colloid & Interface Science, 2013, 193-194(6):24-34.

[3] Mcdonald K J, Choi K S. Chemistry of Materials, 2013, 23(21):4863–4869.

[4] Luo Z, Li C, Zhang D, et al. Chemical Communications, 2015, 52(58):9013.

[5] Hong W, Li L, Xue R, et al. Journal of Colloid & Interface Science, 2017, 485:175-182.

[6] Meidanchi A, Akhavan O. Carbon, 2014, 69(69):230-238.

[7] Liu S, Yu J, Jaroniec M. Chemistry of Materials, 23 (2011) 4085-4093.

[8] Zhang Chen, Nan Zhang, Yi-Jun Xu. CrystEngComm, 2013, 15, 3022-3030.

[9] Xin Z, Li X, Sun H, et al. Applied Materials & Interfaces, 2015, 7(28):15414.

[10] Yang Z, Wan Y, Xiong G, et al. Materials Research Bulletin, 2015, 61:292-297.

[11] Maletin M, Moshopoulou E G, Kontos A G, et al. Journal of the European Ceramic Society, 2007, 27(13–15):4391-4394.